In Vitro Degradation Behavior of Electrospun Polyglycolide, Polylactide, and Poly(lactide-*co*-glycolide)

Young You,[1] Byung-Moo Min,[2] Seung Jin Lee,[3] Taek Seung Lee,[1] Won Ho Park[1]

[1]*Department of Textile Engineering, Chungnam National University, Daejeon 305-764, South Korea*
[2]*Department of Oral Biochemistry, College of Dentistry, Seoul National University, Seoul 110-749, South Korea*
[3]*College of Pharmacy, Ewha Wowans University, Seoul 120-750, South Korea*

Received 17 March 2004; accepted 25 May 2004
DOI 10.1002/app.21116
Published online in Wiley InterScience (www.interscience.wiley.com).

ABSTRACT: The electrospinning of polyglycolide (PGA), poly(L-lactide) (PLA), and poly(lactide-*co*-glycolide) (PLGA; L-lactide/glycolide = 50/50) was performed with chloroform or 1,1,1,3,3,3-hexafluoro-2-propanol (HFIP) as a spinning solvent to fabricate their nanofiber matrices. The morphology of the electrospun PGA, PLA, and PLGA nanofibers was investigated with scanning electron microscopy (SEM). The PLGA nanofibers, electrospun with a nonpolar chloroform solvent, had a relatively large average diameter (760 nm), and it had a relatively broad distribution in the range of 200–1800 nm. On the other hand, the PGA and PLA fibers, electrospun with a polar HFIP solvent, had a small average diameter (~300 nm) with a narrow distribution. This difference in the fiber diameters may be associated with the polarity of the solvent. Also, the *in vitro* degradation of PGA, PLA, and PLGA nanofiber matrices was examined in phosphate buffer solutions (pH 7.4) at 37°C. The degradation rates of the nanofiber matrices were fast, in the order of PGA > PLGA ⩾ PLA. Structural and morphological changes during *in vitro* degradation were investigated with differential scanning calorimetry and wide-angle X-ray diffraction. For the PGA matrix, a significant increase in the crystallinity during the early stage was detected, as well as a gradual decrease during the later period, and this indicated that preferential hydrolytic degradation in the amorphous regions occurred with cleavage-induced crystallization, followed by further degradation in the crystalline region.
 J Appl Polym Sci 95: 193–200, 2005

Key words: degradation; fibers; polyesters

INTRODUCTION

Among biodegradable polymers, polyglycolide (PGA), poly(L-lactide) (PLA), and their random copolymer poly(lactide-*co*-glycolide) (PLGA) have extensive applications as surgical sutures, implant materials, drug carriers, and scaffolds for tissue engineering because they have diverse biodegradability and good mechanical properties and biocompatibility and have received Food and Drug Administration approval for medical devices.[1] Both PGA and PLA (L- or D-form) are partially crystalline, whereas PLGA is amorphous. PLA has a slower degradation rate than PGA because of the hydrophobic methyl group in the backbone. PGA usually has a high degree of crystallinity and is insoluble in many common organic solvents, and this makes the solution processing of PGA very difficult.[2] In contrast, PLA and PLGA can be readily dissolved in common solvents such as chloroform.

Correspondence to: W. H. Park (parkwh@cnu.ac.kr).
Contract grant sponsor: Korean Ministry of Science and Technology.

The mechanism of degradation in PGA, PLA, and PLGA films and sutures (microfibers) in aqueous media has been widely investigated as a function of the time, temperature, crystallinity, and pH level for properties such as the molecular weight and mechanical strength.[3–11] However, the degradation behavior of their nanofibers and nanofiber matrices prepared by electrospinning has been little studied.[2,12] In comparison with films and microfiber nonwovens, a nanofiber matrix has an extremely high specific surface area and high interfiber pores. Therefore, nanofiber matrices electrospun from PLA, PGA, and PLGA have diverse potential applications, such as biomimetic scaffolds for tissue engineering, drug carriers, and sensors.[13–16] For biomedical applications, it is very important to understand the degradation characteristics of nanofiber matrices.

In this study, we compared the *in vitro* degradation behavior of electrospun PGA, PLA, and PLGA nanofiber matrices. For this purpose, we used 1,1,1,3,3,3-hexafluoro-2-propanol (HFIP) for PGA and PLA and chloroform for PLGA as spinning solvents. HFIP could provide thinner fibers than chloroform via electrospinning. The *in vitro* degradation behavior of the electrospun PGA, PLA, and PLGA nanofiber matrices was monitored by weight-loss measurements, differ-

TABLE I
Molecular Weight (*MW*), T_g, and T_m Values of PGA, PLA, and PLGA

	MW	T_g (°C)	T_m (°C)
PLGA	108,000	31	—
PGA	14,000–20,000	42	224
PLA	450,000	64	173

ential scanning calorimetry (DSC), and wide-angle X-ray diffraction (WAXD). In particular, the results for PGA were compared with reported data for a PGA microfiber matrix.

EXPERIMENTAL

Materials

PGA and PLGA (L-lactide/glycolide = 50/50) were purchased from Purac Co. (NE). PLA was purchased from Boehringer Ingelheim (Germany). The molecular weights, glass-transition temperatures (T_g's), and melting temperatures (T_m's) of PGA, PLA, and PLGA are listed in Table I. HFIP and chloroform were purchased from Aldrich Co. (MO) and used as received.

Electrospinning of PGA, PLA, and PLGA solutions

The PGA, PLA, and PLGA solutions were prepared with a solvent (chloroform or HFIP). In the electrospinning process, a high electric potential was applied to a droplet of a blend solution at the tip (inside diameter = 0.495 mm) of a syringe needle, as shown in Figure 1. The optimum concentrations of PGA, PLA, and PLGA solutions for fiber formation were 8, 5 and 15 wt %, respectively, under the following spinning conditions. The electrospun ultrafine fibers were collected on a target, which was placed 7 cm from the syringe tip. A voltage of 17 kV was applied to the collecting target with a high-voltage power supply (Chungpa EMT, Seoul, Korea). The polymer solutions were delivered via a syringe pump to control the mass-flow rate. The mass-flow rate of the solutions was 4 mL/h. All electrospinning was carried out at room temperature.

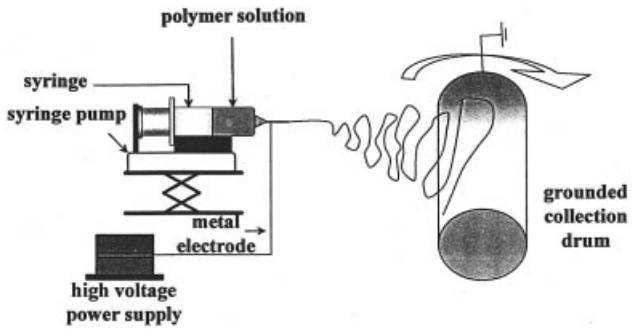

Figure 1 Schematic diagram of the electrospinning equipment.

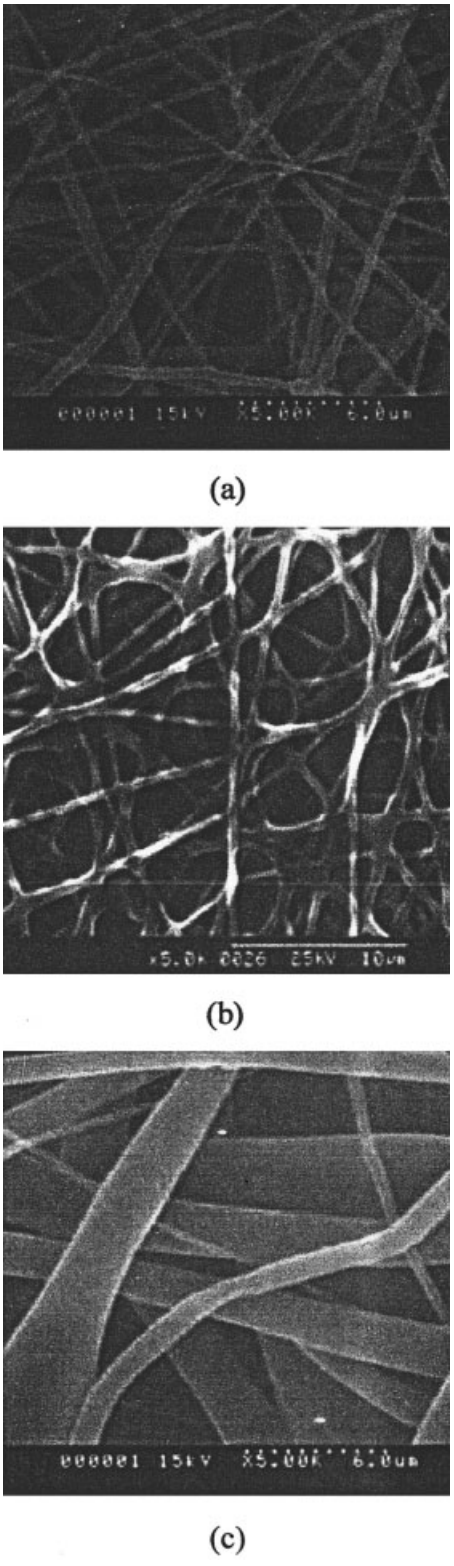

Figure 2 SEM images of electrospun (a) PGA, (b) PLA, and (c) PLGA.

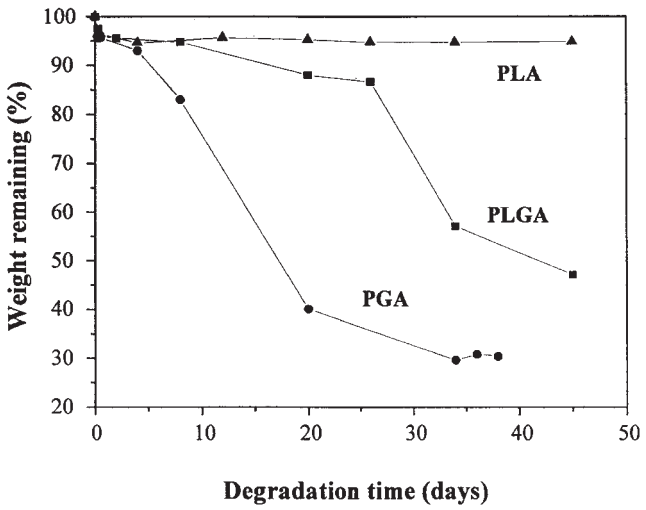

Figure 3 *In vitro* degradation of electrospun PGA, PLA, and PLGA.

In vitro degradation

Electrospun samples were cut into rectangles (40 × 40 × 0.1 mm^3) for *in vitro* degradation testing. The samples were placed in closed bottles containing 40 mL of a phosphate buffer solution (PBS; pH 7.4) and were incubated *in vitro* at 37°C for different times. After each degradation period, the sample was washed, dried in a vacuum oven at room temperature for 24 h, and weighed. The weight-loss percentages of the samples were calculated from the dried weights obtained before and after degradation.

Characterization

The morphology of the nanofiber matrix was observed on a Hitachi (Tokyo, Japan) S-2350 scanning electron microscope after gold coating. The average fiber diameters were determined from an analysis of the SEM im-

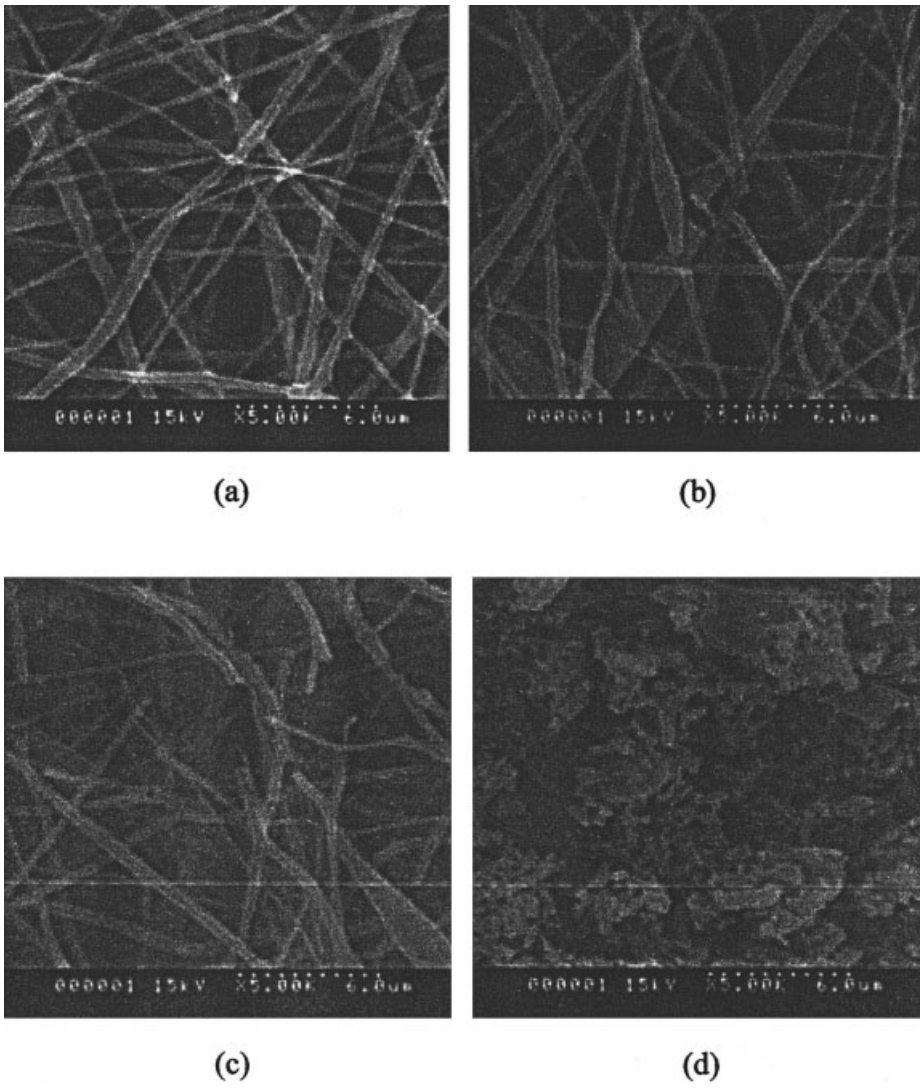

Figure 4 Morphological changes in the electrospun PGA matrix during *in vitro* degradation: (a) 0, (b) 1, (c) 4, and (d) 12 days.

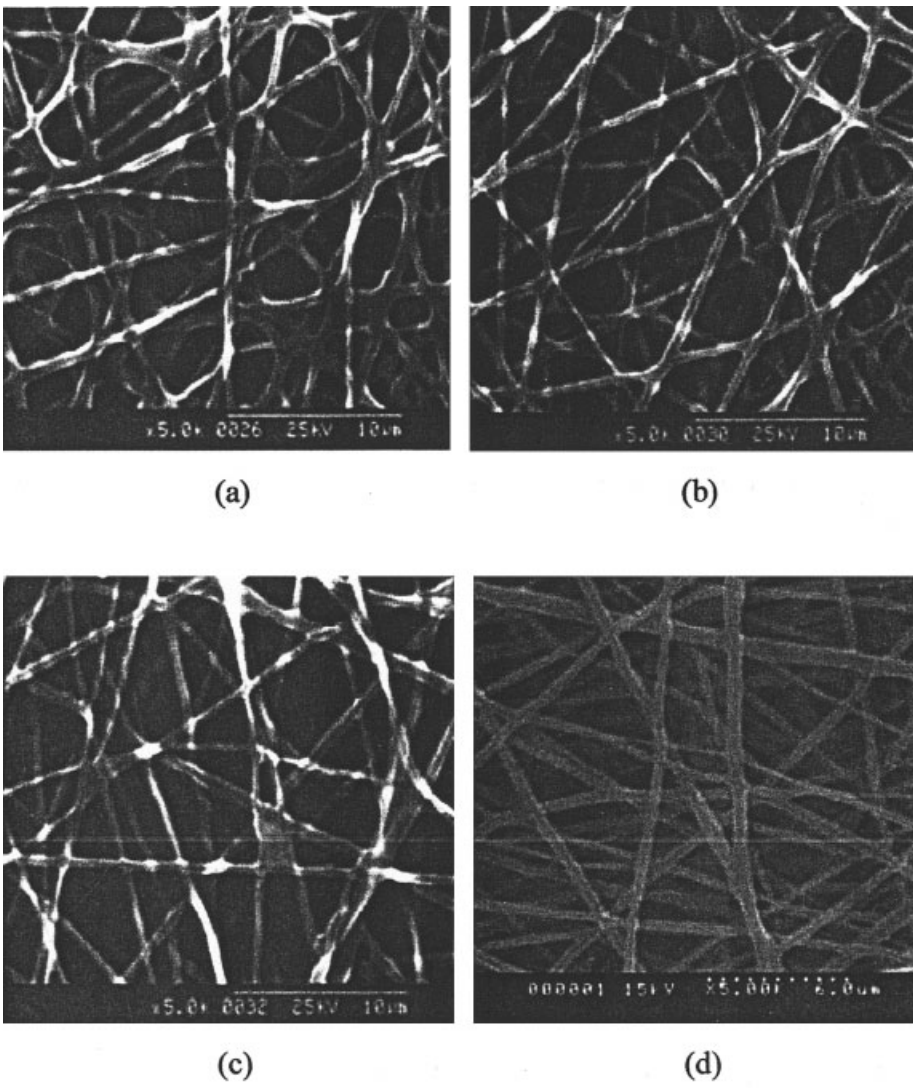

Figure 5 Morphological changes in the electrospun PLA matrix during *in vitro* degradation: (a) 0, (b) 12, (c) 20, and (d) 45 days.

ages with a custom-code image-analysis program. DSC measurements were conducted with a PerkinElmer (MA) DSC7 instrument under a nitrogen atmosphere. About 5-mg samples were sealed in an aluminum pan for the measurements. The samples were heated from 10 to 250°C at a rate of 20°C/min, held at 250°C for 1 min, and then quenched to 10°C. The samples were reheated to 250°C. The crystalline structure of the samples was analyzed on a wide-angle X-ray diffractometer (model D/max-IIB, Rigaku International Corp., Tokyo, Japan).

RESULTS AND DISCUSSION

Morphology of the electrospun PGA, PLA, and PLGA nanofibers

Figure 2 shows SEM micrographs of PGA, PLA, and PLGA nanofibers electrospun from 8, 5 and 15 wt % solutions in HFIP or chloroform, respectively. The average fiber diameter of PGA electrospun at a concentration of 8 wt % was 310 nm, and the fiber diameters were 50–650 nm. The electrospun PLA fibers had values (290 and 100–600 nm) similar to those of the PGA fibers. On the other hand, the PLGA nanofibers electrospun with chloroform had a relatively large average diameter (760 nm), and it had a broad distribution in the range of 200–1800 nm. The solution viscosities and spinning conditions of the PGA, PLA, and PLGA solutions were almost constant. Therefore, we believe that this difference in the fiber diameters may be associated with the polarity of the spinning solvent, that is, the polarity of the solution.

In vitro degradation of the PGA, PLA, and PLGA nanofibers

The degradation of aliphatic polyesters occurs through the simple hydrolysis of the ester backbone

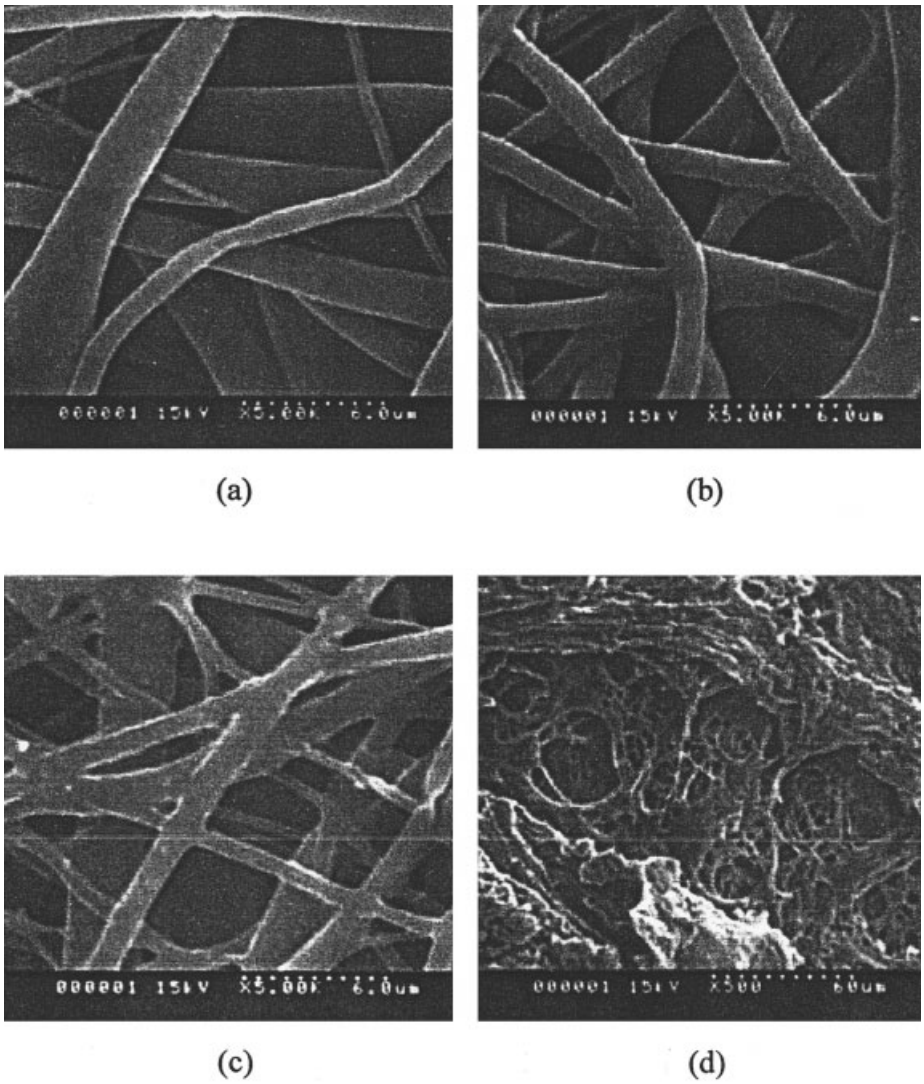

Figure 6 Morphological changes in the electrospun PLGA matrix during *in vitro* degradation: (a) 0, (b) 1, (c) 8, and (d) 20 days.

under aqueous conditions.[8,17,18] The degradation rate depends on the crystallinity, molecular weight, copolymer composition, morphological structure, and so on. Figure 3 shows the weight loss of electrospun PGA, PLA, and PLGA nanofiber matrices. The degradation rate of PGA was higher than that of PLGA. During the first 25 days of degradation, PLGA exhibited a very slow weight-loss rate (this region is sometimes called the induction period). The weight loss was accelerated after this period. At 45 days, the residual weight of PLGA was below 50%. On the contrary, PGA showed a rapid degradation rate without an induction period, unlike PLGA, and a residual weight of approximately 40% at 20 days. PGA had a lower fiber diameter (higher surface area) and molecular weight than PLGA. The attack of water to the polymer backbone under aqueous conditions could occur more quickly in the PGA matrix, although PGA was highly crystalline. Therefore, we believe that the faster degradation of the PGA matrix may have been mainly caused by its higher surface area and/or molecular weight, which overcame the counteracting crystallinity effect. As expected, no significant weight loss of PLA occurred during the degradation for 45 days.

Figures 4–6 illustrate the morphological changes in electrospun PGA, PLA, and PLGA matrices during *in vitro* degradation. Even after 1 day of degradation, some PGA nanofibers broke down [Fig. 4(b)]. A considerable number of the fibers had broken down after 4 days. After 12 days of degradation, the nanofiber matrix of PGA changed into chunks consisting of the short fiber fragments. These separated chunks from the severe degradation of PGA were different from the

porous, membrane-like structure of PLGA (discussed later). Shum and Mak[19] reported on the morphological characterization of a PGA microfiber nonwoven matrix, which has been commercialized as scaffolding for tissue engineering, during *in vitro* degradation (PBS, pH 7.4, and 37°C). A surface defect (microcrack) was observed on PGA microfibers after 3 days, whereas in this study, some PGA nanofibers were broken down after 1 day. The surface defect led to fiber rupture after several days of degradation. This difference in the degradation rates of the nanofiber and microfiber matrices was thought to be attributable to the fiber diameter (surface area).

No significant morphological change in PLA was observed during the degradation for 45 days, as shown in Figure 5. For the PLGA matrix in Figure 6, for the first 4 days of degradation, no significant morphological changes were observed, but after 8 days of degradation, the fibers seemed to be breaking down and partially adhering to one another [Fig. 6(c)]. After 20 days of degradation, the fibrous structure of the PLGA matrix disappeared, and a porous, membrane-like structure, which agglomerated from fragmented chunks, was formed. PLGA is an amorphous polymer and has a T_g (31°C) lower than the degradation temperature (37°C). Therefore, the thermally induced relaxation of polymer chains could occur during degradation. We believe that the porous, membrane-like structure, not separated chunks, may have been caused by shrinkage due to thermally induced relaxation.

Figure 7 shows changes in the DSC thermograms of the PGA and PLA nanofiber matrices during *in vitro* degradation. Although there were slight changes in the DSC thermogram of PLA, the melting endotherms of PGA gradually shifted to lower temperatures with peak broadening. This indicated that the degradation process of PGA occurred in the crystalline region after preferential degradation in the amorphous region. Figure 8 shows the changes in the crystallinity (%) of PGA and PLA during degradation. The crystallinity was determined from the melting enthalpy with heats of fusion of 139 J/g for PGA and 94 J/g for PLA.[19,20] A large increase in the crystallinity for the PGA sample was observed within the first 2 days, and thereafter the crystallinity gradually decreased up to the later stage. In the PGA microfiber matrix, the crystallinity gradually increased up to 14 days during *in vitro* degradation and subsequently decreased at 28 days; this indicated that the degradation of the PGA microfibers was much slower than that of the PGA nanofibers in this study.[19] An increase in the crystallinity during hydrolytic degradation has been previously observed in both PGA and PLA samples.[21–25] Although the increase in the crystallinity was not large, it was significant because very little weight was lost

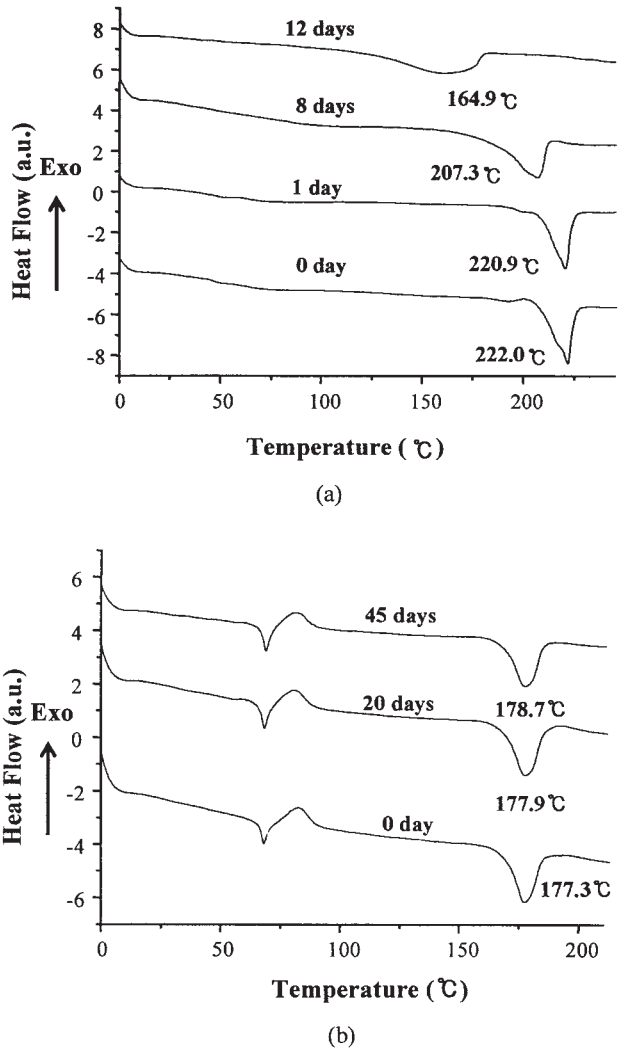

Figure 7 DSC thermograms for electrospun (a) PGA and (b) PLA matrices during *in vitro* degradation.

during the first 2 days. This must have been due to the crystallization of the amorphous region in the early stage of degradation. These observations were explained by cleavage-induced crystallization because the tie chains in the amorphous regions could degrade into fragments; this resulted in a lesser degree of entanglement by the long-chain molecules in the amorphous regions. This behavior was also confirmed by WAXD patterns.

Figure 9 shows WAXD patterns of PGA and PLA nanofiber matrices during *in vitro* degradation. For PGA, two strong reflection peaks, (110) and (020), can be clearly seen; they are located at 22 and 29°, respectively. After 1 day of degradation, the two reflection peaks became stronger. However, the peaks became weak again after 20 days of degradation and then were very weak and broad with an increase in the amorphous halo after 38 days of degradation.

PLA was less crystalline than PGA and had a broad reflection peak (203) at 22°, as shown in Figure 9(b). The reflection peak (200,110) at approximately 16° appeared as a shoulder after 0.25 day. This peak corresponded to the most intense peak of the crystalline poly(L-lactide) or poly(D-lactide) homopolymers. However, no significant changes in the WAXD pattern were observed because the degradation rate of the PLA nanofiber mat was very slow.

CONCLUSIONS

The electrospinning of PGA, PLA, and PLGA (L-lactide/glycolide = 50/50) was performed to fabricate their nanofiber matrices. The PLGA nanofibers electrospun with chloroform had a relatively large average diameter (760 nm) with a relatively broad distribution in the range of 200–1800 nm, whereas the PGA and PLA fibers electrospun with HFIP had a small average diameter (~300 nm) with a narrow distribution. This difference in the fiber diameters could be explained by the polarity of the solvent. Also, the degradation rates of the nanofiber matrices were fast, in the order of PGA > PLGA ⩾ PLA. Structural and morphological changes during *in vitro* degradation were investigated with DSC and WAXD. For the PGA matrix, a significant increase in the crystallinity during the early stage was detected, as well as a gradual decrease during the later period, and this indicated that preferential hydrolytic degradation occurred with cleavage-induced crystallization in the amorphous regions, followed by a further degradation in the crystalline region.

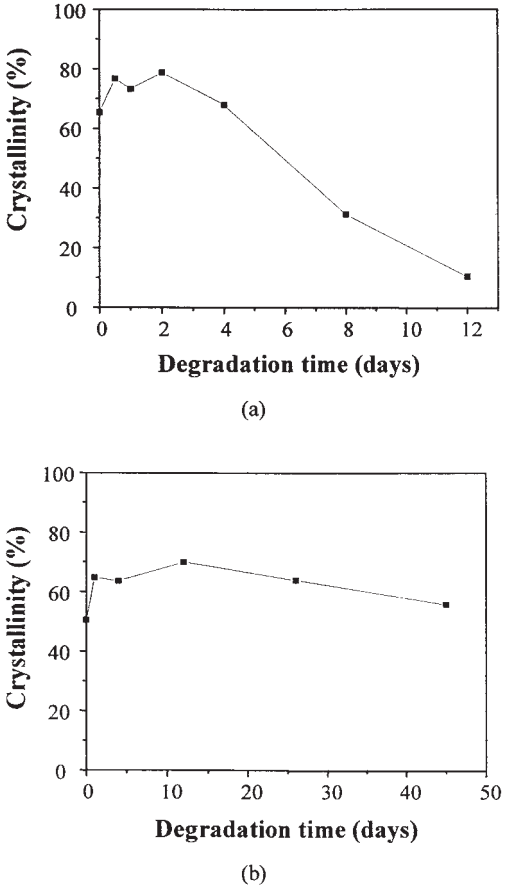

Figure 8 Changes in the crystallinity as a function of the degradation time for electrospun (a) PGA and (b) PLA matrices.

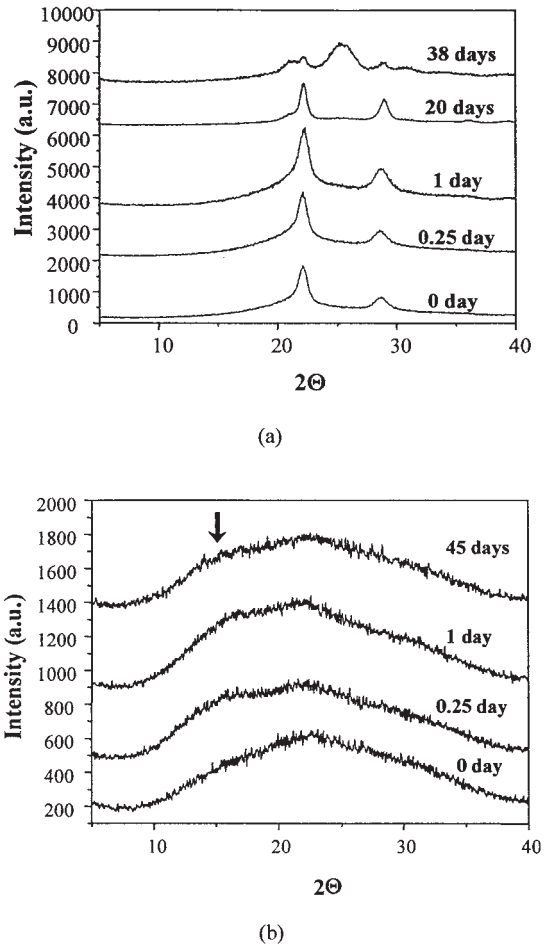

Figure 9 WAXD patterns for electrospun (a) PGA and (b) PLA matrices during *in vitro* degradation.

References

1. Anderson, J. M.; Shiev, M. S. Adv Drug Delivery Rev 1997, 28, 5.
2. Zong, X.; Ran, S.; Kim, K.; Fang, D.; Hsiao, B. S.; Chu, B. Biomacromolecules 2003, 4, 416.
3. Reed, A. M.; Gilding, D. K. Polymer 1981, 22, 494.
4. Gopferich, A. Biomaterials 1996, 17, 103.
5. Miller, N. D.; Williams, D. F. Biomaterials 1984, 5, 365.
6. Chu, C. C. J Biomed Mater Res 1981, 15, 19.
7. Chu, C. C. J Biomed Mater Res 1981, 15, 795.

8. Li, S.; McCarthy, S. Biomaterials 1999, 20, 35.
9. Cohn, D.; Younes, H.; Maron, G. Polymer 1987, 28, 2018.
10. Vert, M.; Mauduit, J.; Li, S. Biomaterials 1994, 15, 1209.
11. Vert, M.; Li, S. M.; Garreau, H. J Controlled Release 1991, 16, 15.
12. Kim, K.; Yu, M.; Zong, X.; Chiu, J.; Fang, D.; Seo, Y.; Hsiao, B. S.; Chu, B.; Hadjiargyrou, M. Biomaterials 2003, 24, 4977.
13. Li, W.; Laurencin, C. T.; Caterson, E. J.; Tuan, R. S.; Ko, F. K. J Biomed Mater Res 2002, 60, 613.
14. Kenawy, E.; Layman, J. M.; Watkins, J. R.; Bowlin, G. L.; Matthews, J. A.; Simpson, D. G.; Wnek, G. E. Biomaterials 2003, 24, 907.
15. Athreya, S. A.; Martin, D. C. Sens Actuators 1999, 72, 203.
16. Wang, X.; Drew, C.; Lee, S.; Senecal, K. J.; Kumar, J.; Samuelson, L. A. Nano Lett 2002, 2, 1273.
17. Schmitt, E. A.; Flanagan, D. R.; Linhardt, R. Macromolecules 1994, 27, 743.
18. Li, S. J Biomed Mater Res 1999, 48, 342.
19. Shum, A. W. T.; Mak, A. F. T. Polym Degrad Stab 2003, 81, 141.
20. Hu, Y.; Hu, Y. S.; Topolkaraev, V.; Hiltner, A.; Baer, E. Polymer 2003, 44, 5681.
21. Zong, X.; Wang, Z.; Hsiao, B. S.; Chu, B.; Zhou, J. J.; Jamiolkowski, D. D.; Muse, E.; Dormier, E. Macromolecules 1999, 32, 8107.
22. Fu, B. X.; Hsiao, B. S.; Chen, G.; Zhou, J.; Koyfman, I.; Jamiolkowski, D. D.; Dormier, E. Polymer 2002, 43, 5527.
23. Lostocco, M. R.; Huang, S. J. Polym Degrad Stab 1998, 61, 225.
24. King, E.; Cameron, R. E. J Appl Polym Sci 1997, 66, 1681.
25. Hurrell, S.; Cameron, R. E. Biomaterials 2002, 23, 2401.